16th Australasian Fluid Mechanics Conference
Crown Plaza, Gold Coast, Australia
2-7 December 2007

Effects of Spin on Tennis Ball Aerodynamics: An Experimental and Computational Study

F. Alam[1], W. Tio[1], S. Watkins[1], A. Subic[1] and J. Naser[2]

[1]School of Aerospace, Mechanical and Manufacturing Engineering
RMIT University, Melbourne, VIC 3083, AUSTRALIA

[2]Faculty of Engineering and Industrial Sciences, Swinburne University, Melbourne, VIC 3122, AUSTRALIA

Abstract

The aerodynamic behaviour of a tennis ball is very complex and significantly differs from other sports balls due to its surface structures (fuzz, seam orientation etc). Relatively high rotational speeds (spin) make the aerodynamic properties of tennis balls even more complex. Although several studies have been conducted on drag and lift in steady state condition (no spin involved) by the author and others, little or no studies have been conducted on spin effects. The so called Magnus effect on a sphere is well known in fluid mechanics. It is believed that the spinning can affect aerodynamic drag and lift of a tennis ball thus the motion and flight path of the ball. Therefore, the primary objectives of this work are to study the spin effects using both experimental and computational methods. In order to achieve these objectives, a series of tennis balls were used to measure their aerodynamics forces as a function of wind speeds, seam orientation and spins. The experimental study was conducted in the RMIT Industrial Wind Tunnel. A computational study of a simplified tennis ball was also studied using commercial software 'FLUENT'. The CFD results were compared with the experimental findings. Flow around the ball was visualised with smoke.

Introduction

The popularity of ball games has been increased significantly and the trend will continue in the near future. Player's individual performance is in the peak form. The International Tennis Federation (ITF) is trying to slow down the speed of the ball as viewers have become bored with not being able to see the ball in flight. This problem is significant with the top ranking male player and some women players. An alternative to reduce the speed of the ball is to introduce a larger ball (with a bigger mass), however, it may change the game itself.. Wilson Rally 2 ball, which is approximately 20% larger diameter compared to Wilson DC 2 or Wilson US Open 3. A study by Alam et al. [3] showed that the larger diameter Wilson Rally 2 has a similar drag coefficient as the normal diameter Wilson DC 2 and Wilson US Open 3. However, the Wilson Rally 2 has a larger overall drag force due to its larger cross sectional area. In the same study, Alam et al. [3] also showed that the Bartlett ball with the similar diameter of Wilson DC 2 and Wilson US Open 3 has the highest drag coefficient (over 20%) over a range of speeds. A visual inspection indicated that the Bartlet ball has a very prominent seam compared to any other ball in its category. The surface structure of a tennis ball is complicated due to the fuzz structure (furry surface) and complex orientation of seam. The aerodynamics properties of tennis balls under steady conditions (no spin involved) have been studied by Alam et al. [1-4], Mehta and Pallis [5], Chadwick [6]. As the ball's flight can be significantly deviated due to spin effects (some player can introduce spin up to 6000 rpm), a comprehensive study by Alam et al. [1-4] has been conducted. Most of these works were experimental. The effects of seam and fuzz are believed to be dominant at a very low speed. It is generally difficult to measure these effects experimentally at these low speeds as instrumental errors are significant. Therefore the primary objective of this work was to study a tennis ball's seam effects on aerodynamic properties using CFD (Computational Fluid Dynamics method) and compare with EFD (Experimental Fluid Dynamics method) findings. As it is very difficult to construct fuzz on a tennis ball, a simplified sphere and sphere with various seam widths was studied to simplify the computational process.

Experimental Facilities, Equipment and the Balls

The aerodynamic forces and their moments were measured for a range of tunnel air speeds and ball types (40 km/h to 140 km/h with an increment of 20 km/h air speeds) as a function of spin rate using a six component force balance in the RMIT University Industrial Wind Tunnel. A mounting device was designed to hold each ball and spin up to 3500 rotation per minute (rpm), see Figure 1. The motorised device was mounted on a 6 component force sensor (type JR-3). Figure 1 shows the experimental set up in the wind-tunnel test section. The distance between the bottom edge of the ball and the tunnel floor was 350 mm, which is well above the tunnel's boundary layer and considered to be out of ground effect. Each ball was tested at spin rates of 500, 1000, 1500, 2000, 2500 and 3000 rpm. Six tennis balls have been selected for this work as they are officially used in the Australian Open Championship. These balls are: Wilson US Open 3, Wilson DC 2, Wilson Rally 2, Slazenger Hydro Guard Ultra Vis 4, Slazenger Hydro Guard Ultra Vis 1, and Bartlett as shown in Fig 3. Their average diameters are: 64.5 mm, 64.5 mm, 69 mm, 65.5 mm, 65.5 mm and 65 mm respectively. The diameter of the ball was determined using an electronic calliper. The width was adjusted so that the ball can slide through the opening with minimum effort. Diameters were measured across several axes and averaged. These balls were brand new. Fuzz structures of these balls were noted to be slightly different from each other. The RMIT University Industrial Wind Tunnel is a closed test section, closed return circuit wind-tunnel. The maximum speed of the tunnel is 145 km/h. The rectangular test section dimension is 3 m (wide) x 2 m (high) x 9 m (long) with a turntable to yaw suitably sized objects. A plan view of the tunnel can be found in the companion paper, Alam and Watkins [7].

Figure 1: A front view of experimental set up in RMIT Industrial Wind tunnel with a motorised supporting device (right)

The ball was spun in relation to vertical axis of the supporting device; hence the side force due to Magnus effect was considered as lift forces. The tunnel was calibrated before conducting the experiments and tunnel's air speeds were measured via a modified NPL ellipsoidal head Pitot-static tube (located at the entry of the test section) connected to a MKS Baratron Pressure sensor through flexible tubing. Purpose made computer software was used to compute all 6 forces and moments (drag, lift, side, yaw moment, pitch moment and roll moment) and their non-dimensional coefficients. During the measurement of forces and moments, the tare forces were removed by measuring the forces on the sting in isolation and them removing them from the force of the ball and sting. Since the blockage ratio was extremely low no corrections were made.

a) Wilson US Open 3 b) Wilson DC 2 c)Wilson Rally 2

d) Slazenger 1 e) Slazenger 4 f) Bartlett

Figure 2: Types of tennis balls used in the study

Computational Fluid Dynamics (CFD) Modelling Procedure

In the computational study, commercial software FLUENT 6.0 was used. In order to understand the simplified model first, a sphere was made using SolidWorks® (see Figure 3). Then two simplified tennis balls without fuzz were also made which are shown in Figures 3 & 4. Two simplified tennis balls were constructed with the following physical geometry: diameter 65 mm, seam with 2 mm width, 1.5 mm depth; and 5 mm width, 1.5 mm depth respectively. All models were then imported to FLUENT 6.0 and GAMBIT was used to generate mesh and refinement. The major consideration when performing the computational analysis is to model a simulation with a reasonable amount of computing resources and accuracy. A control volume was created to simulate the wind tunnel and the ball was placed in the control volume. The control volume (wind tunnel) can be scaled down to reduce the computational cost due to the fact that the full scale wind tunnel was very large with respect to the small size of the tennis ball. Therefore, a reasonable size of domain will be considered to enhance the calculation speed and save the computational time and space. The sphere was used for a benchmark comparison. The dimensions of the reduced scale wind tunnel used are: 2 m long, 1 m wide and 1 m high. A real tennis ball has a textured surface with a convoluted seam (see Figure 2).

Figure 3: Full Sphere 3D CAD Model

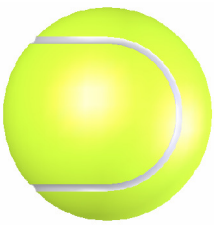

Figure 4: 3D CAD Model of tennis ball with Sim (2 mm w)

In this study only seam effects will be considered as the construction of the filament material (fuzz) of a tennis ball is difficult to construct in CAD and to mesh in CFD. As the accuracy of a CFD solution is governed by the number of cells in a grid, a larger number of cells equates to a better solution, hence better computational power, time and resources are required. However, an optimal solution can be achieved by using fine mesh at locations where the flow is very sensitive and relatively coarse mesh where airflow has little changes. Tetrahedron mesh with mid-edged nodes was used in this study. Figure 5 shows a model of the tennis ball with the tetrahedron mesh. Generally, the structured (rectangular) mesh is preferable to tetrahedron mesh as it gives more accurate results. However, there are some difficulties to use structured mesh in complex geometry. Therefore, in this study, all models were meshed with tetrahedron mesh. The control volume was modelled using GAMBIT. A total of 660,000 hybrid (fine) mesh cells were used for each model. To use fine mesh in the interested areas, sizing function in GAMBIT was used. Mesh validation was done using Examining Mesh command or "Check Volume Meshes" in GAMBIT. The standard k-epsilon model with enhanced wall treatment was used in CFD computational process. Other models were also used to see the variation in solutions and results.

Velocity inlet boundary conditions were used to define flow velocity at the flow inlet. Flow inlet velocities were from 20 km/h to 140 km/h with an increment of 10 km/h up to 40 km/h and thereafter 20 km/h. However, the data for 40 to 140 km/h was presented in this paper in order to compare with the experimental data. The mass flow, the fluxes of momentum, energy, and species through the inlet were estimated using velocity inlet boundary conditions. Apart from the calculations using the velocity inlet above, the rotational speed was introduced to define the rotational movement at the ball. Outflow boundary conditions were used to model flow exits where the details of the flow velocity and pressure were not known prior to solution of the flow problem. Outflow boundary conditions used also needed to satisfy the fully developed flow in order to avoid the backward flow for turbulence flow simulations and convergence solution. The ball was set to be a wall boundary condition to bound fluid and solid regions. Tangential velocity component in terms of the translational or rotational motion of the wall boundary was specified in order to define the rotational movement of the ball. The introduced rotational speed generates the lift force due to the pressure difference between the top and the bottom side of the ball. In this study, the rotational speeds were: 500 rpm to 4000 rpm with an increment of 500 rpm. The rotational speeds were selected such that they can be compared with the experimental findings. The convergence criterion for continuity equations was set to be $1x10^{-5}$ (0.001%).

Figure 5: 3D CAD Model of tennis ball with bigger seam dimension (5 mm w)

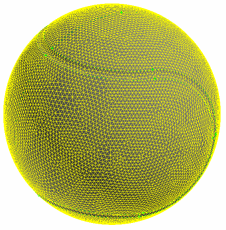

Figure 6: Tennis Ball with Tetrahedral Grid

CFD and Experimental Results

The results for sphere and simplified tennis ball show similar trends and compared well with the published results. The Cd and lift coefficient (c_L) for the sphere under the range of spin conditions were also computed using CFD which are shown in

Figures 7 and 8 respectively. The drag coefficient and lift coefficient for the simplified model (sphere with seam only, no fuzz) are shown in Figures 8 and 11 respectively. With an increase of spin rate, the drag coefficient increases however, the drag coefficient reduces as Reynolds number (wind velocity) increases (see Figures 7 & 8). The reduction of drag coefficients at higher Reynolds numbers is slightly lower compared to lower Reynolds numbers. The lift coefficient also increases with the increase of spin rate and decreases with the increase of Reynolds numbers (see Figures 10 & 11). For higher Reynolds numbers (eg, corresponding to 140 km/h), the reduction of lift coefficients is minimum and the trend of reduction is significantly lower compared to the trend of drag coefficients.

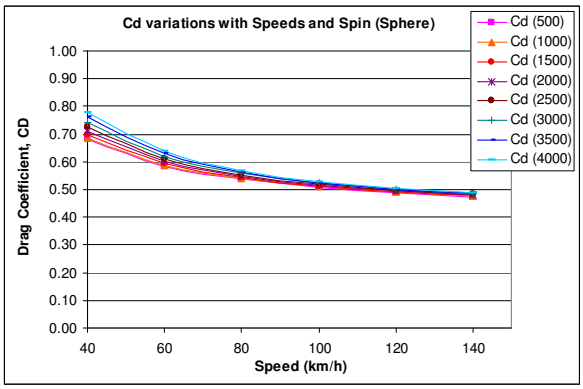

Figure 7: Cd as a function of spin rate and velocity (CFD), sphere

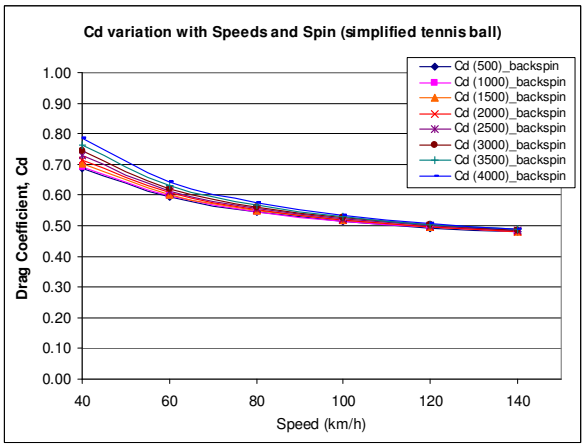

Figure 8: Cd as a function of spin rate and velocity (CFD), simplified tennis ball

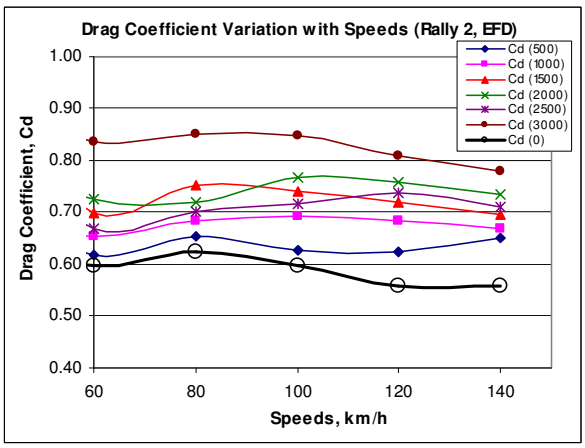

Figure 9: Cd as a function of spin rate and velocity, Wilson Rally 2 tennis ball (EFD)

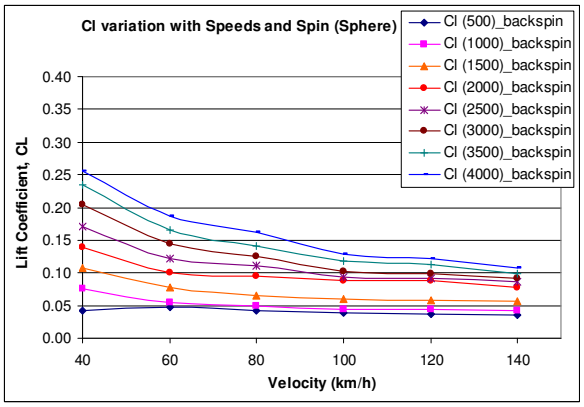

Figure 10: Cl as a function of spin rate and velocity, Sphere (CFD

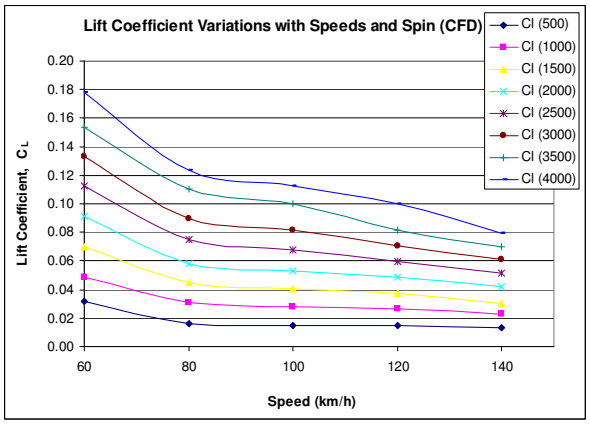

Figure 11: Cl as a function of spin rate and velocity (CFD), simplified tennis ball

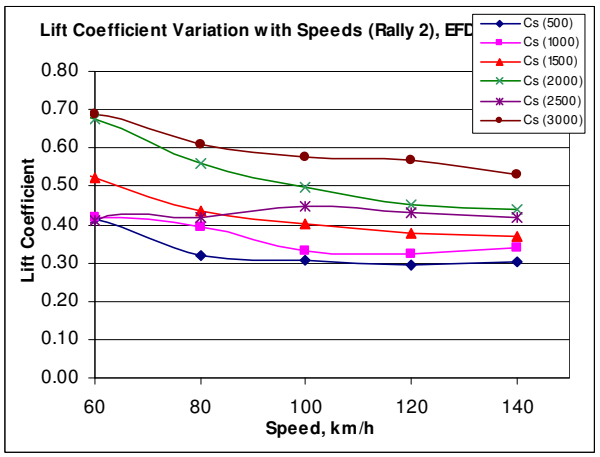

Figure 12: Cl as a function of spin rate and velocity, Wilson Rally 2 tennis ball (EFD)

The plots for the experimentally (EFD) found drag and lift coefficients for Wilson Rally 2 tennis ball are shown in Figures 9 and 12 respectively. In the drag coefficient plot, the drag coefficient of a steady condition (no spin involved) is also shown with a deep dark line to compare with the drag and lift coefficients when spin is involved. As expected, the drag coefficient reduces with an increase of speed. The drag coefficients increase with spin. However, this increase is minimal at high speeds. At low speeds, the drag coefficients are scattered over a wide range and are volatile. Studies by Alam et al. [3, 4] indicated that the drag coefficients at low speeds for steady condition (no spin) are much higher compared to the data at high

speeds. Their finding agreed well with Mehta and Pallis [5]. It is generally difficult to measure accurately the aerodynamic forces and moments at low speeds due to the data acquisition sensitivities. However, for tennis balls, this low speed has a significant influence on the forces and moments as fuzz structures (they are very rough at low speeds) play a dominant role in increasing the aerodynamic drag. With an increase of speed, the fuzz orientation becomes more streamlined and reduces the aerodynamic drag. Mehta and Pallis [5] reported that the fuzz can increase the drag of a tennis ball by up to 40% depending on the Reynolds number. The drag coefficient increases with the increase of spin rate at all speeds tested except for the rotational speed of 2000 rpm. It is larger at low speeds however then reduces significantly at high speeds (see Figure 10). It is not clear at this stage why the drag coefficient at this spin rate is relatively higher at low speeds but is suspected that it is a Reynolds number effect. Efforts are being undertaken to investigate this behaviour.

The lift coefficient increases with the increase of spin rates (see Figure 12). However, the lift coefficient reduces with the increase of wind speeds except the lowest spin (500 rpm). The lift coefficient drops significantly as wind speed increases at high rotational speeds (spins). However, the reduction of lift coefficients is minimal at low rotational speeds with the increase of wind speed. The lift coefficient for 2000 rpm spin rate at low wind speeds is relatively higher compared to 2500 rpm spin rate. A similar trend for the drag coefficients was also noted. However, the variation of lift coefficient between 2000 rpm and 2500 rpm becomes minimal at high wind speeds. One of the reasons for higher drag coefficients of a tennis ball when spun is believed to be the characteristics of the fuzz elements. A close visual inspection of each ball after the spin, it was noted that the fuzz comes outward from the surface and the surface becomes very rough. As a result, it is believed that the fuzz element generates additional drag. However, as the speed increases, the rough surface (fuzz elements) becomes streamlined and reduces the drag. The drag coefficients determined by CFD compared to EFD at low Reynolds numbers are close, however, with the increase of Reynolds numbers, the Cd values are significantly lower. The variation is believed to be due to extreme simplification of the CFD tennis ball (without fuzz). For lift coefficients, a significant variation in magnitudes between the experimental and computational findings is noted. The CFD findings are lower compared to EFD results. However, a similar trend is noted. Again, it is thought to be due to extreme simplification of the CFD tennis ball model.

General Discussions

The CFD results for a sphere and simplified tennis balls indicated no significant variation in drag coefficients, however, a significant variation in the magnitude of lift coefficients is noted (see Figures 7-8, 10-11 and Tables 1 & 2). Both drag and lift coefficients demonstrated similar trends. The drag coefficients by CFD have some variations compared to the experimental results. The lift coefficient (Cl) found by CFD has significant variations in magnitudes compared to the experimental results. However, both CFD and experimental results have shown similar trends.

Table 1: Drag and lift coefficients for a sphere (CFD)

Sphere												
	Backspin		Backspin		Backspin		Back Spin		Backspin		Backspin	
Spin Speed	40 km/h		60 km/h		80 km/h		100 km/h		120 km/h		140 km/h	
rpm	Cd	Cl	Cd	Cl	Cd	Cl	Cd	Cl	Cd	Cl	Cd	Cl
500	0.681	0.042	0.583	0.047	0.539	0.043	0.508	0.038	0.488	0.037	0.471	0.035
1000	0.688	0.075	0.587	0.054	0.540	0.050	0.510	0.045	0.490	0.044	0.475	0.042
1500	0.699	0.107	0.594	0.078	0.543	0.065	0.513	0.060	0.492	0.058	0.479	0.056
2000	0.711	0.140	0.601	0.100	0.547	0.095	0.515	0.089	0.495	0.088	0.481	0.078
2500	0.726	0.172	0.610	0.122	0.552	0.110	0.519	0.093	0.497	0.092	0.485	0.086
3000	0.742	0.205	0.619	0.144	0.558	0.126	0.522	0.101	0.500	0.099	0.486	0.091
3500	0.761	0.235	0.629	0.165	0.562	0.142	0.525	0.118	0.501	0.113	0.487	0.098
4000	0.779	0.255	0.641	0.186	0.566	0.161	0.529	0.129	0.502	0.121	0.489	0.107

Using the standard approximations formula, approximate error of 1.5% in forces coefficients was found both in experimental and computational studies, which can be considered within acceptable limits.

Table 2: Drag and lift coefficients for a simplified tennis ball (CFD)

Simplified Tennis Ball with 5 mm Seam Width												
	Backspin		Backspin		Backspin		Back Spin		Backspin		Backspin	
Spin Speed	40 km/h		60 km/h		80 km/h		100 km/h		120 km/h		140 km/h	
rpm	Cd	Cl	Cd	Cl	Cd	Cl	Cd	Cl	Cd	Cl	Cd	Cl
500	0.686	0.039	0.594	0.062	0.545	0.083	0.514	0.078	0.494	0.077	0.479	0.076
1000	0.693	0.077	0.597	0.079	0.546	0.127	0.516	0.104	0.495	0.100	0.480	0.099
1500	0.702	0.112	0.601	0.113	0.549	0.124	0.518	0.120	0.496	0.110	0.481	0.107
2000	0.714	0.147	0.607	0.149	0.553	0.130	0.520	0.127	0.498	0.116	0.482	0.114
2500	0.728	0.180	0.614	0.182	0.557	0.134	0.523	0.129	0.500	0.119	0.484	0.117
3000	0.745	0.215	0.621	0.202	0.562	0.137	0.526	0.131	0.503	0.124	0.486	0.120
3500	0.764	0.247	0.630	0.246	0.568	0.144	0.530	0.138	0.504	0.126	0.488	0.123
4000	0.785	0.276	0.641	0.250	0.574	0.150	0.535	0.140	0.506	0.129	0.490	0.127

Conclusions and Recommendations for Further Work

The following conclusions are made from the work presented here:

- The spin has significant effects on the drag and lift of a new tennis ball. The averaged drag coefficient is relatively higher compared to the non- spin condition.
- The lift force coefficient increases with spin rate. However, the increase is minimal at the higher speeds.
- The rotational speed can play a significant role at the lower speeds.
- Spin increases the lift or down force depending on the direction of rotation at all speeds. However, the increase is minimal at high speeds.
- A significant variation between CFD and EFD results was found as the complex tennis ball with fuzz elements is extremely difficult to model in CFD
- Although the CFD results cannot be used for experimental validation, they can be used for quantitative values for drag and lift
- In order to improve CFD results accuracy, it is required to model the fuzz element and mesh it correctly

Acknowledgments

Our sincere gratitude and thanks are due to Mr Ian Overend and Mr Jeremy Luci, School of Aerospace, Mechanical and Manufacturing Engineering, RMIT University for their technical assistance with the test rig and experimental set up.

References

[1] Alam, F., Tio, W., Subic, A. and Watkins, S., "An experimental and computational study of tennis ball aerodynamics, *Proceedings of the 3rd Asia Pacific Congress on Sports Technology (APST2007)*, 23-26 September, Singapore, 2007

[2] Alam, F., Subic, A. and Watkins, S., "An experimental study of spin effects on tennis ball aerodynamic properties, *Proceedings of the Asia Pacific Congress on Sports Technology (APST2005)*, pp 240-245, ISBN 0-646-45025-5, 12-16 September, Tokyo, Japan, 2005.

[3] Alam, F., Watkins, S. and Subic, A., "The Aerodynamic Forces on a Series of Tennis Balls", *Proceedings of the 15th Australasian Fluid Mechanics Conference*, University of Sydney, 13-17 December, Sydney, Australia, 2004.

[4] Alam, F., Subic, A. and Watkins, S., "Effects of Spin on Aerodynamic Properties of Tennis Balls", *Proceedings of the 5th International Conference on Sports Engineering (by ISEA),* 13-16 September, pp 83-89, Vol. 1, ISBN 0-9547861-0-6, University of California, Davis, USA, 2004.

[5] Mehta, R. D. and Pallis, J. M. (2001), "The aerodynamics of a tennis ball", *Sports Engineering*, **4** (4), pp 1-13, 2001.

[6] Chadwick, S. G. and Haake, S. J., "The drag coefficient of tennis balls", *The Engineering of Sport: Research, Development and Innovation*, pp 169- 176, Blackwell Science, 2000.

[7] Alam, F. and Watkins, S., "Effects of Crosswinds on Double Stacked Container Wagons", *Proceedings of the 16th Australasian Fluid Mechanics Conference*, 2-7 December, Gold Coast, Australia, 2007.